



Article

Numerical Performance of the Fractional Direct Spreading Cholera Disease Model: An Artificial Neural Network Approach

Saadia Malik

Department of Information Systems, Faculty of Computing and Information Technology—Rabigh, King Abdulaziz University, Jeddah 21589, Saudi Arabia; smalik1@kau.edu.sa

Abstract: The current investigation examines the numerical performance of the fractional-order endemic disease model based on the direct spreading of cholera by applying the neuro-computing Bayesian regularization (BR) neural network process. The purpose is to present the numerical solutions of the fractional-order model, which provides more precise solutions as compared to the integer-order one. Real values based on the parameters can be obtained and one can achieve better results by utilizing these values. The mathematical form of the fractional direct spreading cholera disease is categorized as susceptible, infected, treatment, and recovered, which represents a nonlinear model. The construction of the dataset is performed through the implicit Runge–Kutta method, which is used to lessen the mean square error by taking 74% of the data for training, while 8% is used for both validation and testing. Twenty-two neurons and the log-sigmoid fitness function in the hidden layer are used in the stochastic neural network process. The optimization of BR is performed in order to solve the direct spreading cholera disease problem. The accuracy of the stochastic process is authenticated through the valuation of the outputs, whereas the negligible calculated absolute error values demonstrate the approach's correctness. Furthermore, the statistical operator performance establishes the reliability of the proposed scheme.

Keywords: cholera disease; direct spreading; fractional order; Bayesian regularization; hidden layer; neural network



Citation: Malik, S. Numerical

Performance of the Fractional Direct Spreading Cholera Disease Model: An Artificial Neural Network Approach. *Fractal Fract.* **2024**, *8*, 432. <https://doi.org/10.3390/fractalfract8070432>

Academic Editors: Olumuyiwa James Peter and Kayode Oshinubi

Received: 17 June 2024

Revised: 15 July 2024

Accepted: 19 July 2024

Published: 22 July 2024



Copyright: © 2024 by the author. Licensee MDPI, Basel, Switzerland. This article is an open access article distributed under the terms and conditions of the Creative Commons Attribution (CC BY) license (<https://creativecommons.org/licenses/by/4.0/>).

1. Introduction

Infectious diseases produce huge numbers of causalities based on the reports of the World Health Organization (WHO) [1]. Appropriate care must be given in order to stop the propagation of these transmissible illnesses through the use of an efficient regulation system. Poor hygienic and interactions with affected or susceptible individuals can lead to a variety of illnesses that are transmissible. Certain infectious illnesses are aqueous-borne, including severe watery diarrhea or cholera, while a few of them are airborne, including tuberculosis and the common cold [2]. Due to insufficient hygiene and the use of polluted water, cholera, as a minor intestinal disease, is prevalent in underdeveloped nations, such as Africa, Asia, and the central or southern parts of the Americas [3]. Within one to two weeks, cholera bacteria are excreted through the feces and can spread to other individuals via polluted food or drink [4]. The Gram-negative microbe *Vibrio cholerae* (VC), a bacterium is found in water environments, is the source of the severe diarrheal illness known as cholera [5]. The most common symptoms of cholera are low blood pressure, severe vomiting, an irregular heartbeat, watery stools, and dry mouth [6]. Both direct and indirect modes of spread are possible [7]. Through physical contact, biting, and genital contact, asymptomatic individuals can spread cholera to others via direct contact. Conversely, cholera is indirectly spread from the atmosphere to humans, when polluted water and food contain VC [8].

Mathematical models are considered a significant tool in order to examine the control and spread of infectious diseases [9]. The progression of infectious illnesses, their effects, and potential future projections of their spread can all be better understood due

to mathematical epidemiology. These systems are applied in the evaluation, implementation, planning, comparison, control, and optimization of numerous detection, therapy, and prevention measures [10]. There are a number of mathematical systems based on cholera that have been designed by different scholars. Codeco [11] proposed two regulation strategies, while primarily focusing on the widespread nature of cholera. A conventional mathematical system based on the management of cholera has been presented by Fatima et al. [6]. Additional investigations based on mathematical cholera models have been presented by Sweileh [9], Fakai [7], Wang et al. [12], and Beryl et al. [3]. The use of mathematical systems is not only limited to cholera; they have abundant applications in computer virus models [13,14], prey–predator systems [15,16], food chain models [17], environmental/economic models [18], human balancing models [19], language learning models [20], and hepatitis B virus models [21].

This study presents numerical solutions of the fractional-order (FO) endemic disease model using direct spreading through the neuro-computing Bayesian regularization (BR) neural network. While there exist various methodologies for the solution of FO endemic disease models, such as the Runge–Kutta method and the usage of neural networks, these have various limitations. However, neural networks also present some advantages in modeling.

Neural networks are able to handle nonlinear and complex relations in data, which enables them to capture underlying patterns in datasets that might be overlooked by other methodologies.

Additionally, neural networks provide a flexible scheme to solve systems of fractional form, where obtaining analytical solutions may be difficult. By applying neural networks, in addition to more traditional methods of solving FO endemic disease models, researchers can obtain valuable insights into datasets. The stochastic process has been used to solve various schemes, while the process based on the BR neural network has not been applied previously to solve FO endemic disease models of direct spreading.

Different mathematical techniques are employed in numerical models, especially when modeling systems with dynamic behavior. A Caputo derivative is a type of fractional derivative that extends the idea of an integer-order derivative to non-integer (fractional) orders. Memory impacts are intrinsic to fractional derivatives, which means that the system's history determines its present condition.

Ordinary differential equations (ODEs), on the other hand, include derivatives of integers that explain the connections between the function itself and its derivatives. The evolution of the system is solely dependent upon its present state; prior conditions have no impact on the current condition of the model.

To present various phenomena based on diseases, the mathematical form of the fractional-order (FO) derivatives is frequently applied. These systems are employed to identify the FO derivatives that exhibit memory influences, extending the use of traditional differential models. To model the dynamics of disease propagation, they require the application of fractional types of differential systems. The purpose of using FO derivatives is to achieve precise and practical solutions. The minute details of superslow development and superfast transition are explored in FO systems, which yields information about the mechanisms and behavior through the use of fractional calculus (FC). FC is applied in the framework of mechanics to calculate indices. Depending on the studied circumstances, the derivative-based FO operator can be significantly better than the integer-order one. By applying the derivative-based FO operator to real-world scenarios, the system's effectiveness has been verified. Furthermore, a great deal of research has been conducted on the derivatives of FO to address a variety of problems, including engineering, mathematics, control networks, and physics. Throughout the past three decades, a number of significant procedures have been used to execute FC in an extensive manner. Each operator is significant and valuable in its own capacity. However, the definition of the CD is most commonly applied to address both non-homogeneous and homogeneous starting points. With regard to implementation, the CD is thought to be simpler than other formulations. By using the

CD, the numerical performance of the model (2) is examined in this study. Some novel points of this work are presented as follows:

- The numerical solutions of the FO direct spreading cholera disease model are presented through the neuro-computing BR neural network process;
- The FO derivative based on the CD is used to present more reliable solutions of the mathematical model;
- Three cases based on FO values between 0 and 1 are presented to solve the mathematical model given in system (2);
- The direct spreading cholera disease model is a nonlinear system that contains four different categories, while the numerical solutions are obtained through the BR neural network;
- A fitness function based on the sigmoid function is presented by taking twenty-two neurons in the hidden layer to obtain the results of the FO model;
- The correctness of the solver is authenticated through the matching of the outcomes and absolute error (AE).

This paper is organized as follows: Section 2 shows the mathematical formulation, Section 3 describes the methodology, Section 4 presents the results and the discussion of the FO model, and the conclusions are listed in Section 5.

2. Mathematical Formulation

The mathematical model contains a population size equal to the total human population, which is further categorized into susceptible $S(x)$, infected $I(x)$, treated $T(x)$, and recovered $R(x)$ groups. $S(x)$ individuals are those who are not infected; however, they can become infected in the future. $I(x)$ individuals are those who exhibit some cholera symptom and can spread the disease. The $T(x)$ category represents those who receive treatment at time x after contracting cholera. $R(x)$ denotes those who recover from cholera and acquire temporary immunity. The integer-order form of the model is given as [22]

$$\begin{cases} \frac{dS(x)}{dx} = \pi - (\mu + \alpha I(x))S(x) + \delta R(x), & S(0) = i_1, \\ \frac{dI(x)}{dx} = \alpha S(x)I(x) - (\tau + \mu + \sigma)I(x), & I(0) = i_2, \\ \frac{dT(x)}{dx} = \sigma I(x) - (g + \gamma + \mu)T(x), & T(0) = i_3, \\ \frac{dR(x)}{dx} = \gamma T(x) - (\delta + \mu)R(x), & R(0) = i_4, \end{cases} \quad (1)$$

where the susceptible population increases through the recovered class at δ rate after losing their temporary immunity with a recruitment rate π . However, this population declines due to environmental factors, with a mortality rate μ , and such individuals migrate to the infected group, which has a rate α . The α rate expands the population throughout the infected class, whereas the σ rate causes the population to decline due to natural causes, cholera, and transfer to the treated group. The rate of mortality caused by cholera is τ , and the individuals who carry the cholera disease are denoted by g . The general population in the treated sector grows over the infected sector with the medication rate σ and shrinks with the recuperation rate γ along with the natural mortality rate μ . In the recovered group, the population grows at rate γ due to its recovery, but, at rate δ , due to immunity loss and natural mortality, the numbers will decline. The population size N is normalized to 1. x denotes the time. The initial conditions (ICs) are i_1 , i_2 , i_3 , and i_4 . The model structure is described in Figure 1.

The FO endemic disease model based on the direct spreading of cholera is presented as

$$\begin{cases} \frac{d^\rho S(x)}{dx^\rho} = \pi - (\mu + \alpha I(x))S(x) + \delta R(x), & S(0) = i_1, \\ \frac{d^\rho I(x)}{dx^\rho} = \alpha S(x)I(x) - (\tau + \mu + \sigma)I(x), & I(0) = i_2, \\ \frac{d^\rho T(x)}{dx^\rho} = \sigma I(x) - (g + \gamma + \mu)T(x), & T(0) = i_3, \\ \frac{d^\rho R(x)}{dx^\rho} = \gamma T(x) - (\delta + \mu)R(x), & R(0) = i_4, \end{cases} \quad (2)$$

where ρ denotes the Caputo derivative (CD), which is given as [23]

$$\frac{d^\rho}{dy^\rho} f(y) = \frac{1}{\Gamma(m-\rho)} \int_0^y (y-\zeta)^{m-\rho-1} f^{(m)}(\zeta) d\zeta \quad (3)$$

ρ represents the fractional-order values and is provided by the user. Values between 0 and 1 have been selected.

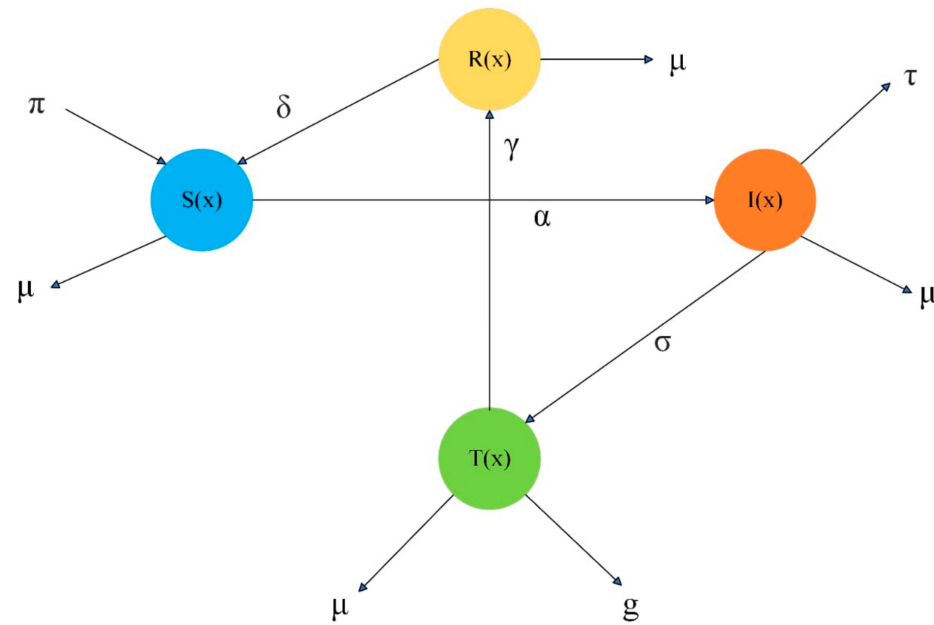


Figure 1. A model based on the direct spreading of cholera.

3. Materials and Methods

The current section describes the procedure based on the BR neural network to obtain the numerical solutions of the FO endemic disease model of direct spreading.

BR Procedure

The BR procedure is one of the schemes that is implemented in statistical modeling and machine learning in order to integrate the prior information about the parameters of the learning model. It utilizes Bayesian implication (BI) principles using regularization techniques to enhance the generalization of the system in order to avoid the problems of overfitting. Bayesian implication, also called Bayesian inference, is an inferential method used to generate subjective probability statements about population parameters by pooling together non-sample data (also called “prior” data) and sample data [24]. Meanwhile, regularization theory poses that the solution of an ill-posed problem is obtainable from a variational principle [25]. BR serves to prevent the problem of overfitting by integrating previous information about the parameters of the model. This scheme also provides an uncertainty estimation related to the model predictions, which offers information for the risk evaluation and decision-making. To integrate the uncertainty of the parameters of regularization, BR automatically regulates the complexity of the system in order to fit the data. This scheme solves a number of challenges as it is suitable for the computational operation of large-scale models. Some implementation procedures of BR are presented as follows.

BI: This is a probabilistic structure for perception under ambiguity. This procedure permits one to upgrade the parameters of the system using experiential data. In this procedure, the parameters are preserved as arbitrary variables along with the related distributions of the probability.

Regularization: This is one of the schemes that is implemented to avoid the problem of overfitting. It reduces overly intricate systems to obtain simpler results. Some of the general regularization schemes are L_1 , L_2 , and elastic net.

Hyperparameter Tuning: In the process of BR, hyperparameters based on the strength of regularization must be identified. Hyperparameter tuning is conducted through the usage of empirical Bayesian cross-validation.

BR is used in data training by taking the previous information about the parameters of the network, including biases or weights. These parameters are updated by using the principles of BI in the training. In the process of BR, prior allocations are identified for the parameters of the network in order to encode the prior assumptions. Currently, BR has been used in various applications, some of which include the estimation of the price of uranium, the estimation of the probability of defaults, highly accurate user-friendly energy audit platforms, feature-based quality classification for the ultrasonic welding of carbon-fiber-reinforced polymers, and the classification of high-dimensional noisy Gaussian mixtures [26,27]. Figure 2 shows the workflow diagram, including the mathematical model, neural structure, and performance results.

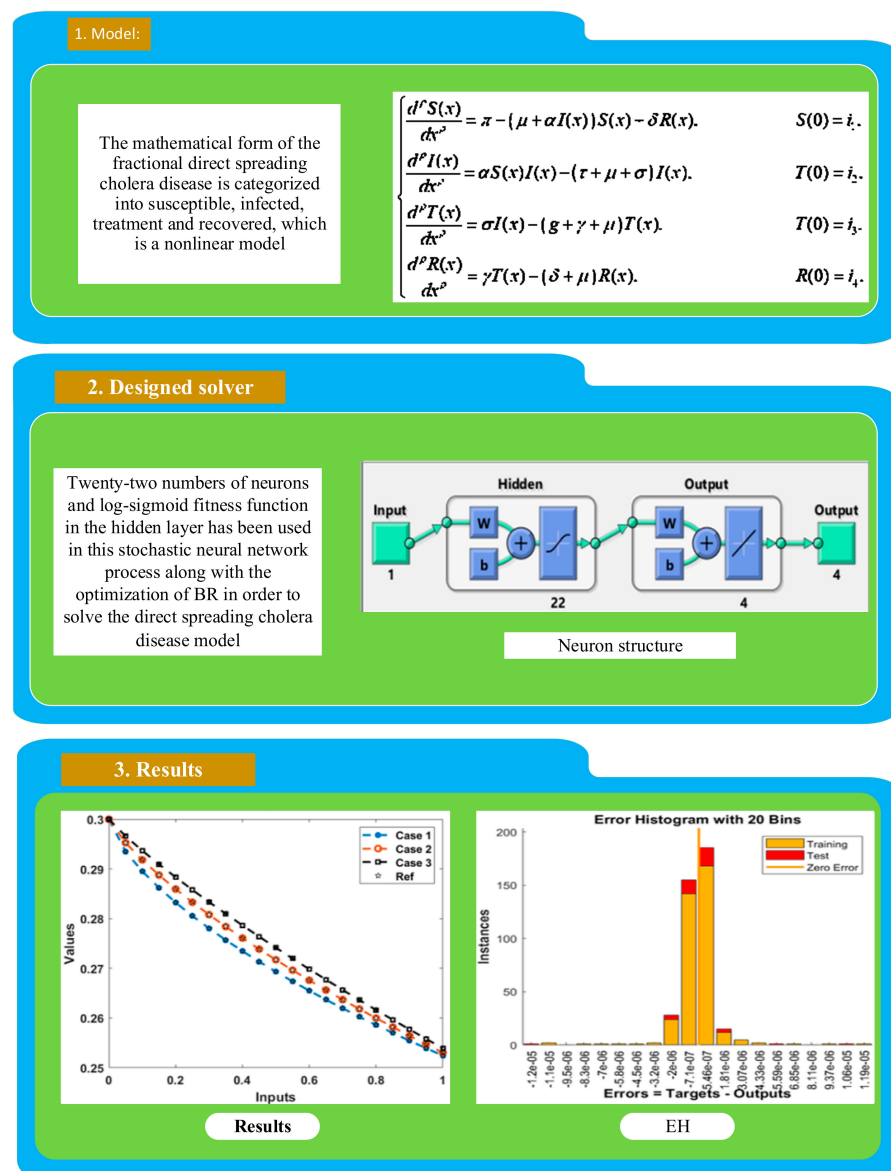


Figure 2. Workflow diagram of the FO endemic disease model based on direct spreading.

The proposed neural network structure for the direct spreading of cholera model is provided by taking 22 neurons. If smaller numbers of neurons are taken, premature convergence and underfitting can occur. However, using more neurons can occasionally result in overfitting, even if it additionally offers outstanding precision. The division of the data is achieved by taking 74% for training and 8% for both validation and testing. Lower training percentages, between 45% and 55%, are used to analyze the mean square error (M.S.E.), which typically shows poor performance. On the other hand, higher precision is attained if the training percentage is greater than 70%. The layer structure of the direct spreading of cholera model is presented in Figure 3.

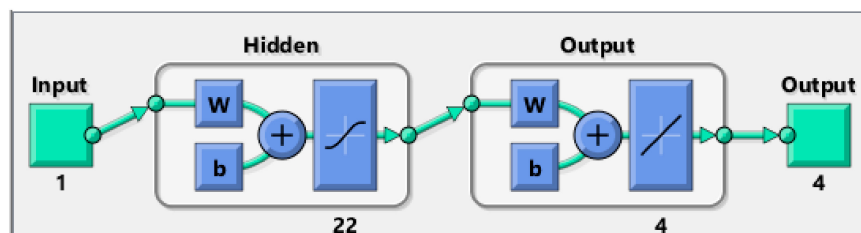


Figure 3. The layer structure.

4. Results

The numerical performance of the direct spreading of cholera model is presented in this section by taking three different cases of the model depending on the FO values. These cases are based on values selected from [22]. The basic aim is to solve this model using supervised neural networks based on the neuro-computing Bayesian regularization neural network process. In the future, real values of the parameters can be substituted in place of these parameters and the model can be solved using the outlined scheme.

Case 1: Consider that the FO value is taken as 0.7 in system (2) and the other parameter values are $\pi = 0.0013$, $\mu = 2.5 \times 10^{-5}$, $\alpha = 0.011$, $\delta = 0.003$, $\tau = 0.015$, $\sigma = 0.115$, $g = 0.04$, and $\gamma = 0.2$, while the ICs are 0.1, 0.2, 0.3, and 0.4 [22].

$$\begin{cases} \frac{d^{0.7}S(x)}{dx^{0.7}} = 0.0013 - (2.5 \times 10^{-5} + 0.011I(x))S(x) + 0.003R(x), & S(0) = 0.1, \\ \frac{d^{0.7}I(x)}{dx^{0.7}} = 0.011S(x)I(x) - 0.130025I(x), & I(0) = 0.2, \\ \frac{d^{0.7}T(x)}{dx^{0.7}} = 0.115I(x) - 0.240025T(x), & T(0) = 0.3 \\ \frac{d^{0.7}R(x)}{dx^{0.7}} = 0.2T(x) - 0.003025R(x), & R(0) = 0.4. \end{cases} \quad (4)$$

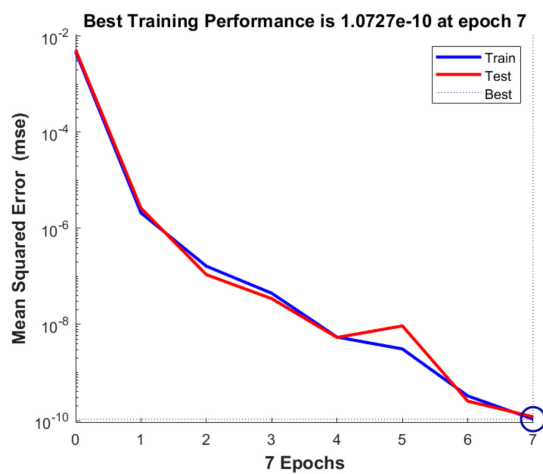
Case 2: Consider that the FO value is taken as 0.8 in system (2) and the other parameter values are $\pi = 0.0013$, $\mu = 2.5 \times 10^{-5}$, $\alpha = 0.011$, $\delta = 0.003$, $\tau = 0.015$, $\sigma = 0.115$, $g = 0.04$, and $\gamma = 0.2$, while the ICs are 0.1, 0.2, 0.3, and 0.4 [22].

$$\begin{cases} \frac{d^{0.8}S(x)}{dx^{0.8}} = 0.0013 - (2.5 \times 10^{-5} + 0.011I(x))S(x) + 0.003R(x), & S(0) = 0.1, \\ \frac{d^{0.8}I(x)}{dx^{0.8}} = 0.011S(x)I(x) - 0.130025I(x), & I(0) = 0.2, \\ \frac{d^{0.8}T(x)}{dx^{0.8}} = 0.115I(x) - 0.240025T(x), & T(0) = 0.3 \\ \frac{d^{0.8}R(x)}{dx^{0.8}} = 0.2T(x) - 0.003025R(x), & R(0) = 0.4. \end{cases} \quad (5)$$

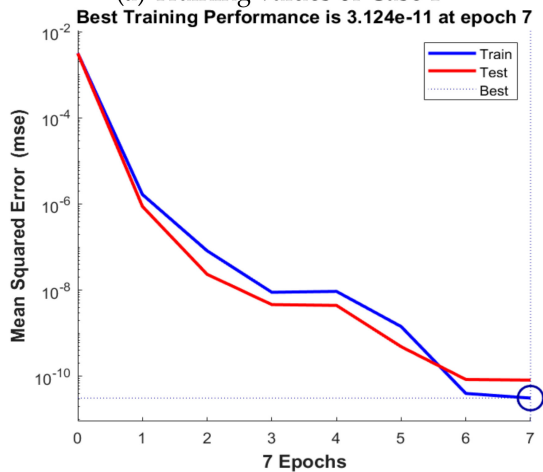
Case 3: Consider that the FO value is taken as 0.9 in system (2) and the other parameter values are $\pi = 0.0013$, $\mu = 2.5 \times 10^{-5}$, $\alpha = 0.011$, $\delta = 0.003$, $\tau = 0.015$, $\sigma = 0.115$, $g = 0.04$, and $\gamma = 0.2$, while the ICs are 0.1, 0.2, 0.3, and 0.4 [22].

$$\begin{cases} \frac{d^{0.9}S(x)}{dx^{0.9}} = 0.0013 - (2.5 \times 10^{-5} + 0.011I(x))S(x) + 0.003R(x), & S(0) = 0.1, \\ \frac{d^{0.9}I(x)}{dx^{0.9}} = 0.011S(x)I(x) - 0.130025I(x), & I(0) = 0.2, \\ \frac{d^{0.9}T(x)}{dx^{0.9}} = 0.115I(x) - 0.240025T(x), & T(0) = 0.3 \\ \frac{d^{0.9}R(x)}{dx^{0.9}} = 0.2T(x) - 0.003025R(x), & R(0) = 0.4. \end{cases} \quad (6)$$

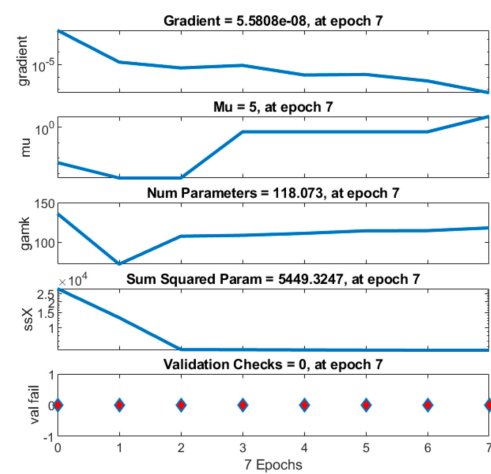
Figures 4–8 show the numerical simulations of the direct spreading cholera model using a BR neural network. Figure 4a–c show the best training and transition state (TS) performance. The purpose of training the dataset is to achieve negligible values of the M.S.E. through training and testing. The best training values are achieved as 1.07270×10^{-10} , 3.12398×10^{-10} , and 2.76863×10^{-12} at epoch 7 for each case. Figure 4d–f illustrate the gradient performance, with values of 5.5808×10^{-8} , 1.5977×10^{-8} , and 1.1257×10^{-8} when solving the direct spreading cholera model. These calculations show the accuracy of the proposed BR neural network for the direct spreading cholera model. The fitting function performance is shown in Figure 5a–c based on the overlapping of the solutions. Figure 5d–f present the values of the error histogram (EH), which are observed as 3.18×10^{-6} , 2.08×10^{-6} , and 5.46×10^{-7} for the respective cases. Figures 6–8 show the regression measures for the direct spreading cholera model in Cases 1 to 3. The regression coefficient value is obtained as 1 for each case, which indicates a perfect model. The best values during testing and training are provided in Table 1.



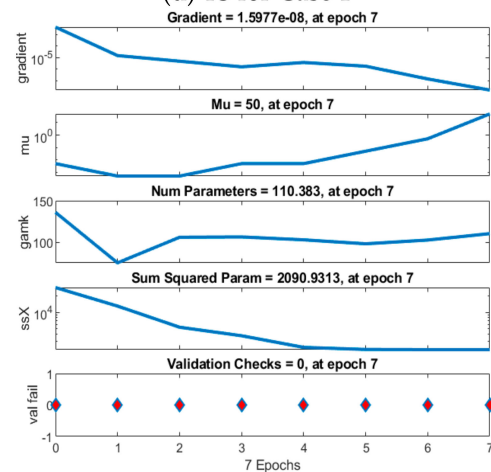
(a) Training values of Case 1



(b) Training values of Case 2

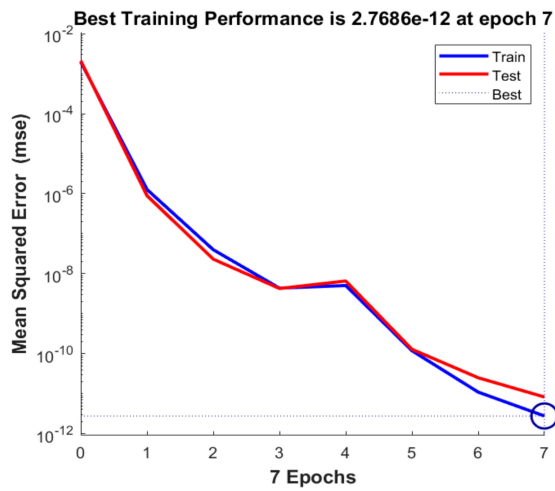


(d) TS for Case 1

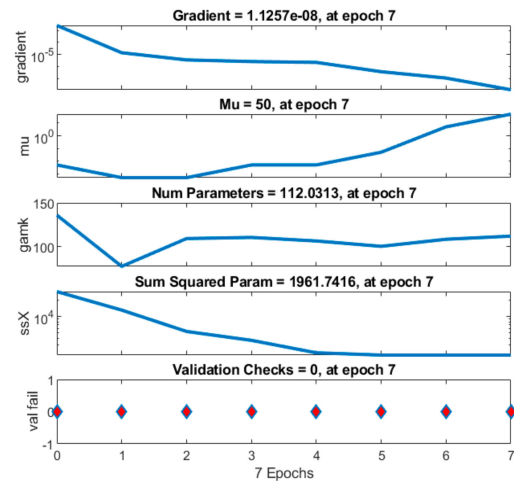


(e) TS for Case 2

Figure 4. Cont.

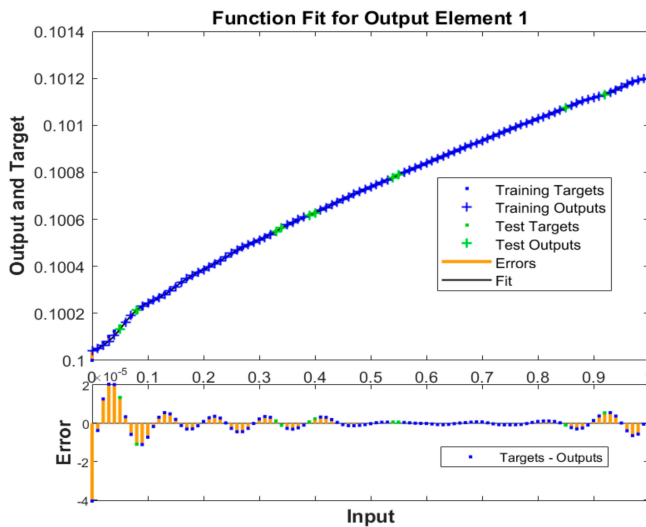


(c) Training values of Case 3

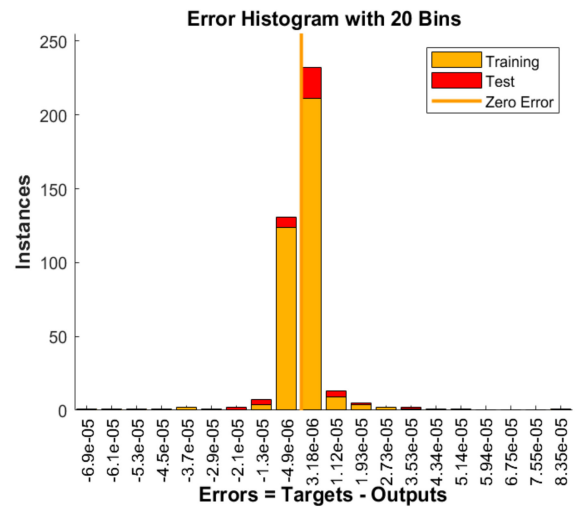


(f) TS for Case 3

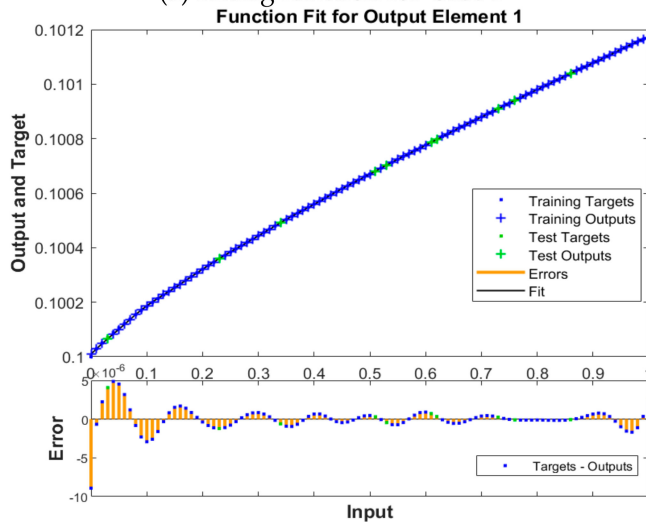
Figure 4. Training and TS performance for Cases 1 to 3 of the direct spreading cholera model.



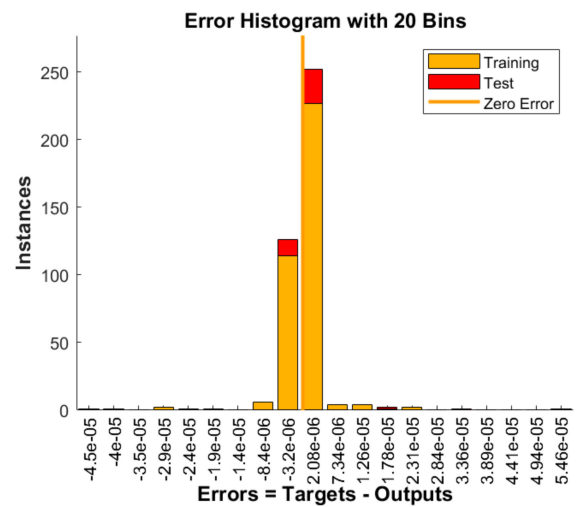
(a) Fitting function for Case 1



(d) EH values of Case 1

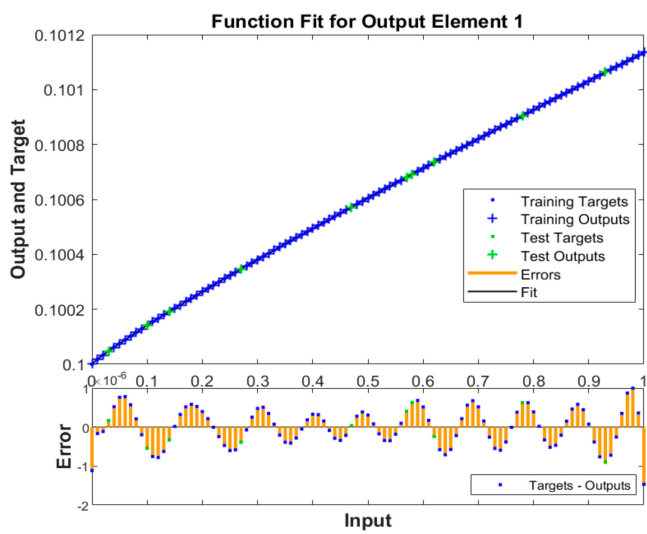


(b) Fitting function for Case 2

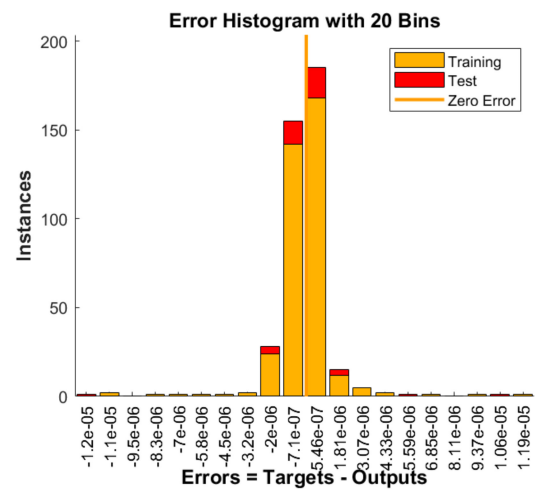


(e) EH values of Case 2

Figure 5. Cont.



(c) Fitting function for Case 3



(f) EH values of Case 3

Figure 5. Fitting function and EH values for Cases 1 to 3 of the direct spreading cholera model.

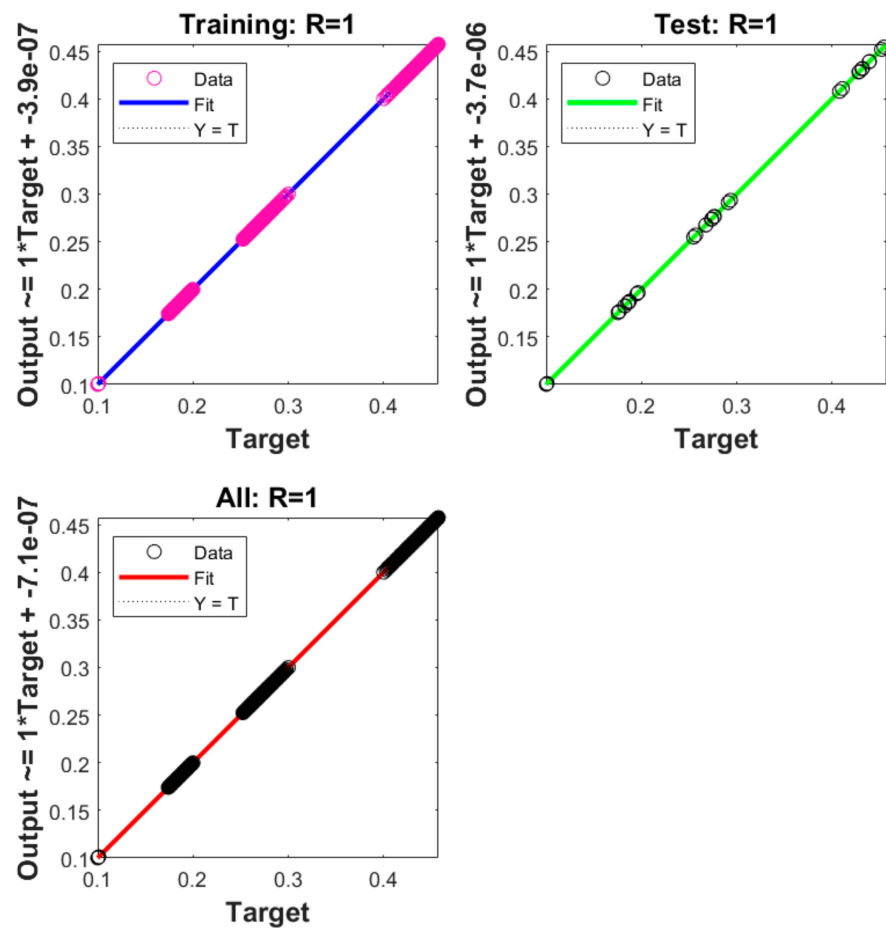


Figure 6. Regression measures for the direct spreading cholera model (1).

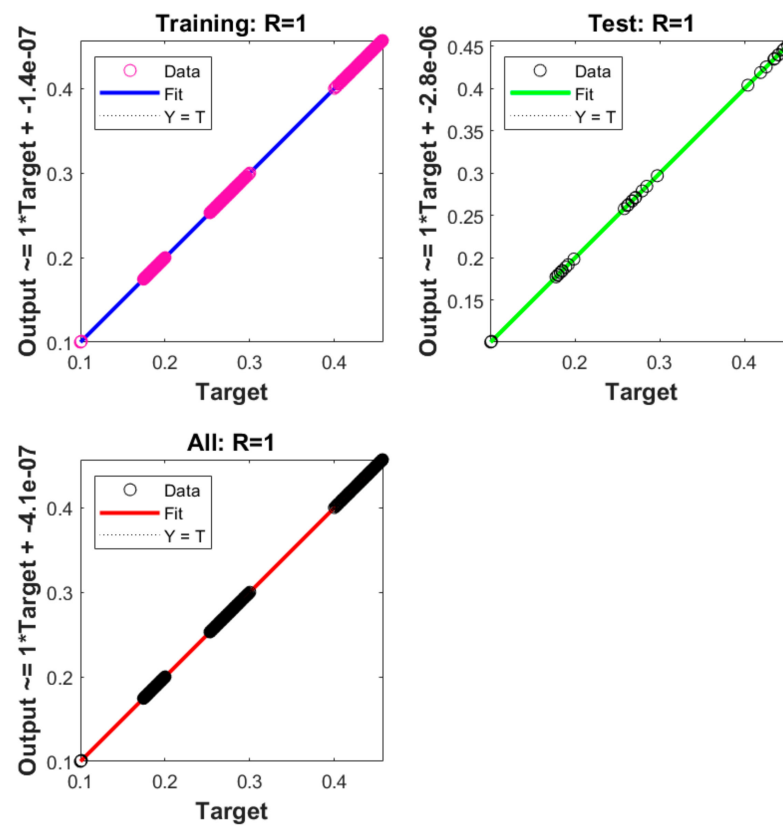


Figure 7. Regression measures for the direct spreading cholera model (2).

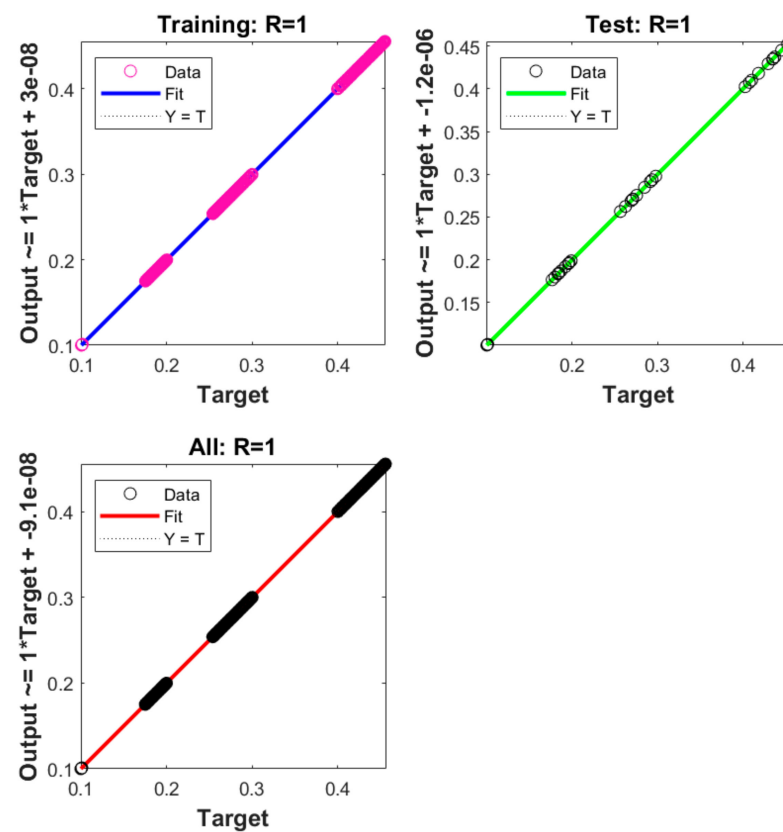


Figure 8. Regression measures for the direct spreading cholera model (3).

Table 1. Best training values for the direct spreading cholera model.

Case	M.S.E.		Performance	Gradient	Iterations	Time
	Test	Train				
1	1.20103×10^{-10}	1.07270×10^{-10}	1.07×10^{-10}	5.58×10^{-8}	07	1 s
2	8.16973×10^{-11}	3.12398×10^{-11}	3.12×10^{-11}	1.60×10^{-8}	07	1 s
3	8.25530×10^{-12}	2.76863×10^{-12}	2.77×10^{-12}	1.13×10^{-8}	07	1 s

Figures 9 and 10 show a comparison of the solutions and AE values for each case of the direct spreading cholera model. Overlapping is achieved in Figure 9, which shows the correctness of the solver. Figure 10 presents the AE values for each class of the model; for class $S(x)$, they are 10^{-5} to 10^{-6} , 10^{-6} to 10^{-7} , and 10^{-6} to 10^{-8} for Cases 1 to 3 of the model. For the category $I(x)$, the AE values are found to be 10^{-4} to 10^{-6} , 10^{-5} to 10^{-6} , and 10^{-6} to 10^{-8} for Cases 1 to 3 of the direct spreading cholera model. For the categories $T(x)$ and $R(x)$, the AE values are calculated as 10^{-5} to 10^{-6} , 10^{-5} to 10^{-7} , and 10^{-6} to 10^{-7} for Cases 1 to 3 of the direct spreading cholera model. These negligible and reducible AE results indicate the precision of the proposed BR neural network when used to solve the direct spreading cholera model.

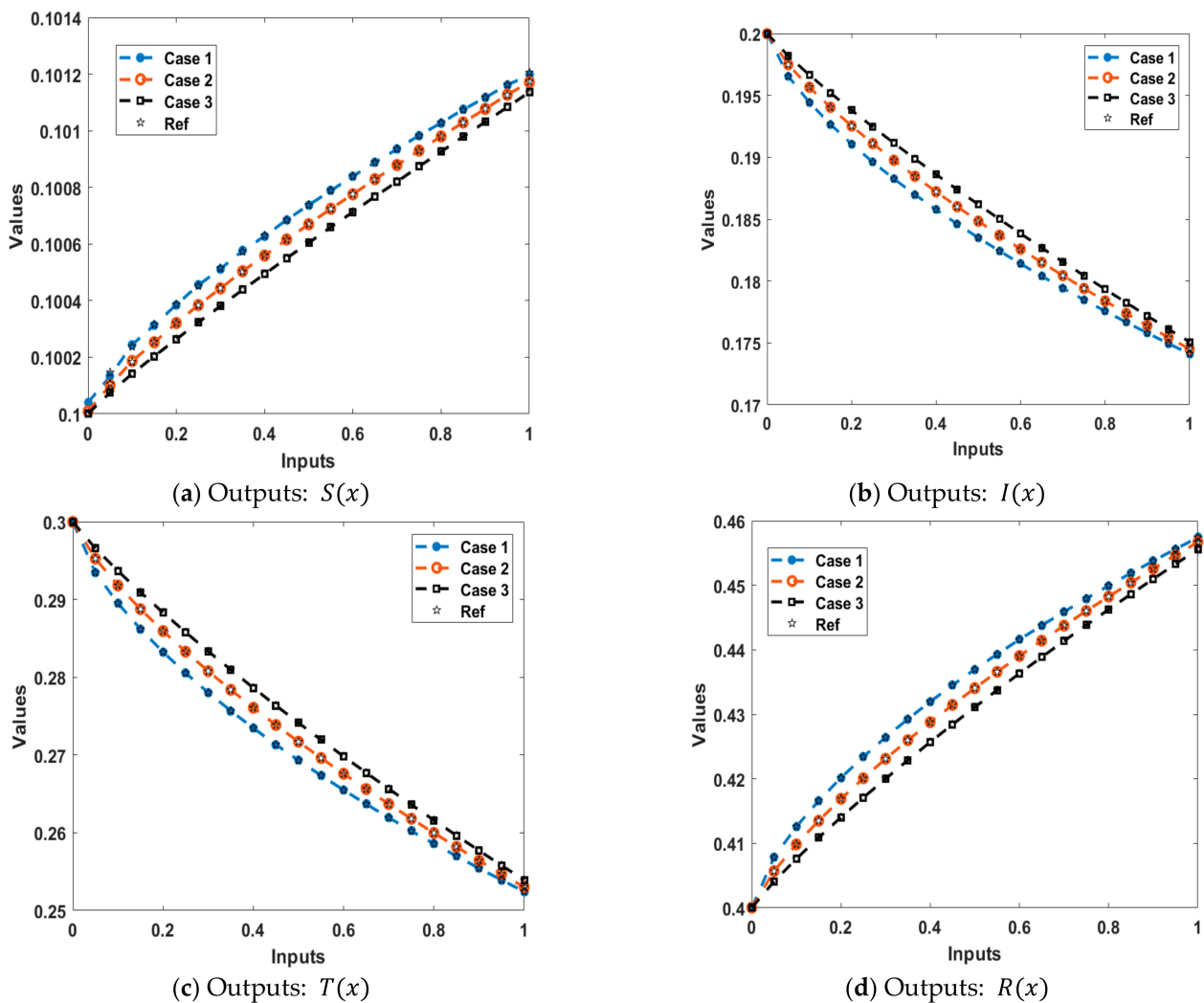


Figure 9. Comparison of the results for the solution of the direct spreading cholera model.

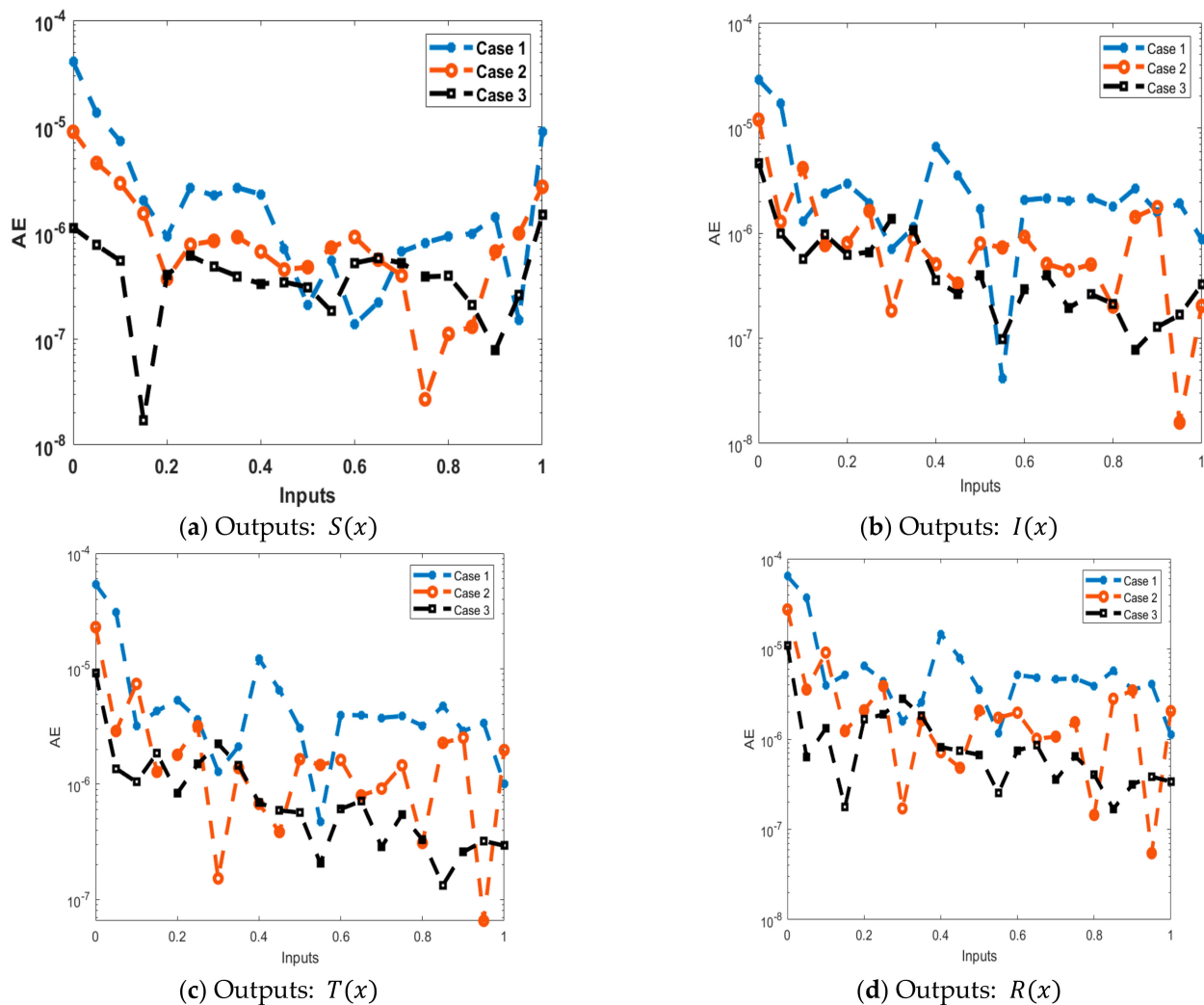


Figure 10. AE values for each class of the direct spreading cholera model.

5. Conclusions

In this work, the numerical performance of the FO endemic disease model based on the direct spreading of cholera has been presented. A neuro-computing BR process has been presented to solve the FO endemic disease model based on the direct spreading of cholera. The mathematical model is categorized into susceptible, infected, treatment, and recovered, which is a nonlinear model. Some of the conclusions of this study are presented as follows.

- The solutions of the FO endemic disease model based on the direct spreading of cholera have been successfully obtained by applying the proposed structure method.
- The aim was to implement the FO derivatives for the precise solution of the model as compared to the integer-order case.
- A dataset has been constructed through the implicit Runge–Kutta method, which is used to reduce the M.S.E., by using 74% of the data for training, while 8% is used for both validation and testing.
- Twenty-two neurons and the log-sigmoid fitness function in the hidden layer have been used via the stochastic neural network process.
- Optimization has been performed through the BR scheme in order to solve the direct spreading cholera disease model.
- The accuracy of the BR stochastic process has been authenticated through the valuation of the outputs, along with a negligible AE.

- The FO values of 0.7, 0.8, and 0.9 have been used in three cases, and the value of 0.9 is found to be more precise as compared to other two cases.

In the future, the proposed neuro-computing BR process can be used to solve susceptible, infected, and recovered models [28,29]; host viral dynamical models [30,31]; and pine wilt disease models [32–34].

Funding: This research work was funded by the Institutional Fund Projects under grant no. (IFPIP: 683-865-1443).

Data Availability Statement: The original contributions presented in the study are included in the article, further inquiries can be directed to the author.

Acknowledgments: The author gratefully acknowledges the technical and financial support provided by the Ministry of Education and King Abdulaziz University, DSR, Jeddah, Saudi Arabia under grant no. (IFPIP: 683-865-1443).

Conflicts of Interest: The author declares no conflicts of interest.

References

1. Brooks, S.; Weston, D.; Greenberg, N. Psychological impact of infectious disease outbreaks on pregnant women: Rapid evidence review. *Public Health* **2020**, *189*, 26–36. [[CrossRef](#)] [[PubMed](#)]
2. Chowdhury, F.; Ross, A.G.; Islam, T.; McMillan, N.A.J.; Qadri, F. Diagnosis, Management, and Future Control of Cholera. *Clin. Microbiol. Rev.* **2022**, *35*, e0021121. [[CrossRef](#)] [[PubMed](#)]
3. Beryl, M.; George, L.; Fredrick, N. Mathematical Analysis of A Cholera Transmission Model Incorporating Media Coverage. *Int. J. Pure Appl. Math.* **2016**, *111*, 219–331. [[CrossRef](#)]
4. Helmi, A.M.; Mukti, A.T.; Soegianto, A.; Effendi, M.H. A review of vibriosis in fisheries: Public health importance. *Syst. Rev. Pharm.* **2020**, *11*, 51–58.
5. Lopez, A.L.; Dutta, S.; Qadri, F.; Sovann, L.; Pandey, B.D.; Bin Hamzah, W.M.; Memon, I.; Iamsirithaworn, S.; Dang, D.A.; Chowdhury, F.; et al. Cholera in selected countries in Asia. *Vaccine* **2020**, *38*, A18–A24. [[CrossRef](#)]
6. Fatima, S.; Krishnarajah, I.; Jaffar, M.; Adam, M.B. A Mathematical Model for the Control of Cholera in Nigeria. *Res. J. Environ. Earth Sci.* **2014**, *6*, 321–325. [[CrossRef](#)]
7. Fakai, S.A.; Ibrahim, M.O.; Siddiqui, A.M. A deterministic mathematical model on cholera dynamics and some control strategies. *Int. J. Sci. Eng. Technol.* **2014**, *8*, 1115–1118.
8. Bakare, E.A.; Hoskova-Mayerova, S. Optimal Control Analysis of Cholera Dynamics in the Presence of Asymptomatic Transmission. *Axioms* **2021**, *10*, 60. [[CrossRef](#)]
9. Sweileh, W.M. Global research activity on mathematical modeling of transmission and control of 23 selected infectious disease outbreak. *Glob. Health* **2022**, *18*, 4. [[CrossRef](#)]
10. Siettos, C.I.; Russo, L. Mathematical modeling of infectious disease dynamics. *Virulence* **2013**, *4*, 295–306. [[CrossRef](#)]
11. Codeço, C.T. Endemic and epidemic dynamics of cholera: The role of the aquatic reservoir. *BMC Infect. Dis.* **2001**, *1*, 1. [[CrossRef](#)]
12. Wang, J.; Wang, J. Analysis of a reaction–diffusion cholera model with distinct dispersal rates in the human population. *J. Dyn. Differ. Equ.* **2021**, *33*, 549–575. [[CrossRef](#)]
13. Sabir, Z.; Raja, M.A.; Mumtaz, N.; Fathurochman, I.; Sadat, R.; Ali, M.R. An investigation through stochastic procedures for solving the fractional order computer virus propagation mathematical model with kill signals. *Neural Process. Lett.* **2023**, *55*, 1783–1797. [[CrossRef](#)]
14. Sabir, Z.; Baleanu, D.; Raja, M.A.Z.; Alshomrani, A.S.; Hincal, E. Meyer wavelet neural networks procedures to investigate the numerical performances of the computer virus spread with kill signals. *Fractals* **2023**, *31*, 2340025. [[CrossRef](#)]
15. Umar, M.; Sabir, Z.; Raja, M.A.Z. Intelligent computing for numerical treatment of nonlinear prey–predator models. *Appl. Soft Comput.* **2019**, *80*, 506–524. [[CrossRef](#)]
16. Umar, M.; Sabir, Z.; Raja, M.A.Z.; Amin, F.; Saeed, T.; Sanchez, Y.G. Design of intelligent computing solver with Morlet wavelet neural networks for nonlinear predator–prey model. *Appl. Soft Comput.* **2023**, *134*, 109975. [[CrossRef](#)]
17. Sabir, Z. Stochastic numerical investigations for nonlinear three-species food chain system. *Int. J. Biomath.* **2022**, *15*, 2250005. [[CrossRef](#)]
18. Chen, Q.; Sabir, Z.; Raja, M.A.Z.; Gao, W.; Baskonus, H.M. A fractional study based on the economic and environmental mathematical model. *Alex. Eng. J.* **2023**, *65*, 761–770. [[CrossRef](#)]
19. AbuAli, N.; Sabir, Z. Designing a heuristic computing structure to solve the human balancing model. *J. King Saud Univ.-Comput. Inf. Sci.* **2024**, *36*, 101890. [[CrossRef](#)]
20. Sabir, Z.; Ben Said, S.; Al-Mdallal, Q. An artificial neural network approach for the language learning model. *Sci. Rep.* **2023**, *13*, 22693. [[CrossRef](#)]
21. Umar, M.; Sabir, Z.; Raja, M.A.Z.; Baskonus, H.M.; Ali, M.R.; Shah, N.A. Heuristic computing with sequential quadratic programming for solving a nonlinear hepatitis B virus model. *Math. Comput. Simul.* **2023**, *212*, 234–248. [[CrossRef](#)]

22. Tilahun, G.T.; Woldegerima, W.A.; Wondifraw, A. Stochastic and deterministic mathematical model of cholera disease dynamics with direct transmission. *Adv. Differ. Equ.* **2020**, *2020*, 670. [[CrossRef](#)]
23. Rezapour, S.; Etemad, S.; Mohammadi, H. A mathematical analysis of a system of Caputo–Fabrizio fractional differential equations for the anthrax disease model in animals. *Adv. Differ. Equ.* **2020**, *2020*, 481. [[CrossRef](#)]
24. Western, B.; Jackman, S. Bayesian Inference for Comparative Research. *Am. Political-Sci. Rev.* **1994**, *88*, 412–423. [[CrossRef](#)]
25. Girosi, F.; Jones, M.; Poggio, T. Regularization Theory and Neural Networks Architectures. *Neural Comput.* **1995**, *7*, 219–269. [[CrossRef](#)]
26. Sariev, E.; Germano, G. Bayesian regularized artificial neural networks for the estimation of the probability of default. *Quant. Financ.* **2020**, *20*, 311–328. [[CrossRef](#)]
27. Marcos, F.L.; Plangklang, B. A high accurate user-friendly energy audit platform of a university building using ANN Bayesian regularization and Levenberg-Marquardt algorithm. *Energy Rep.* **2024**, *11*, 2220–2235. [[CrossRef](#)]
28. Ahmad, Z.; Bonanomi, G.; Cardone, A.; Iuorio, A.; Toraldo, G.; Giannino, F. Fractalfractional sirs model for the disease dynamics in both prey and predator with singular and nonsingular kernels. *J. Biol. Syst.* **2024**, 1–34. [[CrossRef](#)]
29. Umar, M.; Sabir, Z.; Raja, M.A.Z.; Sánchez, Y.G. A stochastic numerical computing heuristic of SIR nonlinear model based on dengue fever. *Results Phys.* **2020**, *19*, 103585. [[CrossRef](#)]
30. Lu, H.; Giannino, F.; Tartakovsky, D.M. Parsimonious models of in-host viral dynamics and immune response. *Appl. Math. Lett.* **2023**, *145*, 108781. [[CrossRef](#)]
31. Junswang, P.; Sabir, Z.; Raja, M.A.Z.; Salahshour, S.; Botmart, T.; Weera, W. An Advanced Stochastic Numerical Approach for Host-Vector-Predator Nonlinear Model. *Comput. Mater. Contin.* **2022**, *72*, 5823–5843. [[CrossRef](#)]
32. Ahmad, Z.; Bonanomi, G.; di Serafino, D.; Giannino, F. Transmission dynamics and sensitivity analysis of pine wilt disease with asymptomatic carriers via fractal-fractional differential operator of Mittag-Leffler kernel. *Appl. Numer. Math.* **2023**, *185*, 446–465. [[CrossRef](#)]
33. Yusuf, A.; Acay, B.; Mustapha, U.T.; Inc, M.; Baleanu, D. Mathematical modeling of pine wilt disease with Caputo fractional operator. *Chaos Solitons Fractals* **2021**, *143*, 110569. [[CrossRef](#)]
34. Khan, M.A.; Ullah, S.; Okosun, K.O.; Shah, K. A fractional order pine wilt disease model with Caputo–Fabrizio derivative. *Adv. Differ. Equ.* **2018**, *2018*, 410. [[CrossRef](#)]

Disclaimer/Publisher’s Note: The statements, opinions and data contained in all publications are solely those of the individual author(s) and contributor(s) and not of MDPI and/or the editor(s). MDPI and/or the editor(s) disclaim responsibility for any injury to people or property resulting from any ideas, methods, instructions or products referred to in the content.